Supplement of Atmos. Meas. Tech., 15, 2177–2198, 2022
https://doi.org/10.5194/amt-15-2177-2022-supplement

Atmospheric Measurement Techniques
Open Access
EGU

Supplement of

Controlled-release experiment to investigate uncertainties in UAV-based emission quantification for methane point sources

Randulph Morales et al.

Correspondence to: Dominik Brunner (dominik.brunner@empa.ch)

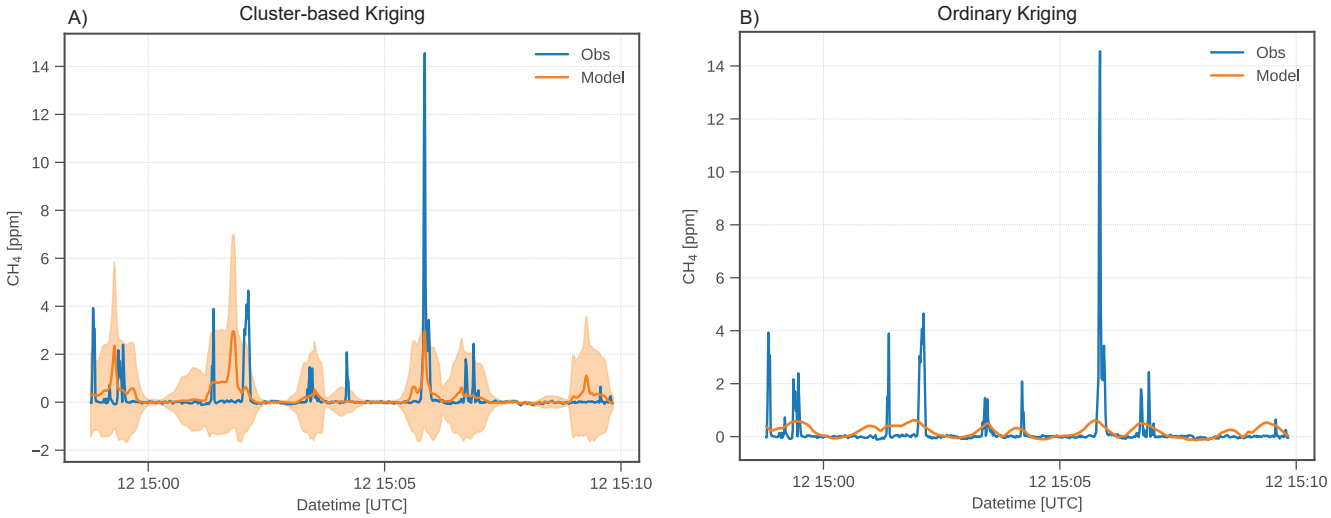

Figure S1. Reconstructed timeseries of flight 312_03 extracted from the produced A) cluster-based kriging field and B) ordinary kriging field compared to the original timeseries of methane measurements. Orange shade areas indicate the uncertainty produced by kriging.

Fig. S7 illustrates the difference between the reconstructed emission plume for flight 312_03 from QCLAS measurements using the cluster-based kriging vs. ordinary kriging. The figure on the upper left is the obtained emission plume using the cluster-based kriging. The figure on the middle left is the obtained emission plume using ordinary kriging. Figure on the upper right is the obtained background methane field and middle right is the methane field from the elevated cluster. To test whether the only difference between the cluster-based approach over ordinary kriging is the length-scale component alone, we forced our ordinary kriging approach to use length scales similar to that of the cluster-kriging approach. The resulting emission plume using ordinary kriging with length scales similar to the cluster approach are showed in the lower left plot in Fig. S7. This shows that the absence of membership probability of the background and elevated cluster in the ordinary kriging tends to produce noisier emission fields. The noise in the emission field resulted to a 10 % decrease in emission estimate.

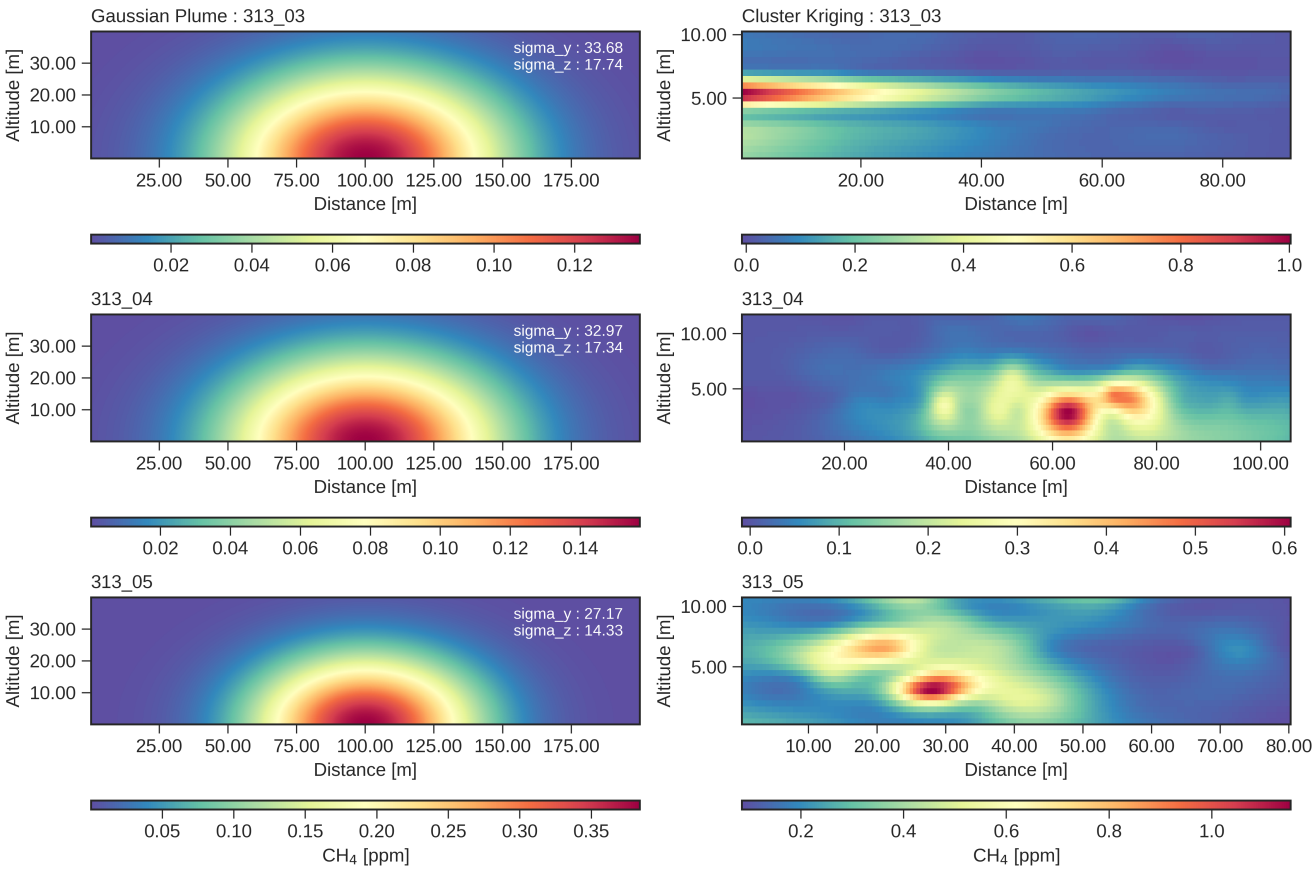

Figure S2. Vertical cross-section from downwind distance of more than 100 m of methane molar fractions using a theoretical Gaussian dispersion model and cluster-kriging estimated prediction

Table S1. Summary of emission estimates

Date	Flight Code	Rel. rate [gs^{-1}]	Cluster Kriging			Ordinary Kriging		
			Proj. wind	Sca. wind	Log. wind	Proj. wind	Sca. wind	Log. wind
23-Feb	223_01*	0.48 ± 0.04	0.64 ± 0.56	0.66 ± 0.41	0.56 ± 0.40	1.29 ± 0.98	1.26 ± 0.69	0.85 ± 0.70
24-Feb	224_01	0.29 ± 0.03	0.79 ± 0.66	0.76 ± 0.49	0.82 ± 0.51	0.60 ± 0.48	0.61 ± 0.30	0.61 ± 0.31
25-Feb	225_01*	0.29 ± 0.03	0.28 ± 0.48	0.31 ± 0.41	0.29 ± 0.42	0.30 ± 0.24	0.30 ± 0.11	0.29 ± 0.11
	225_02*	0.29 ± 0.03	0.41 ± 0.46	0.45 ± 0.34	0.42 ± 0.36	0.44 ± 0.33	0.45 ± 0.14	0.44 ± 0.15
	225_03*	0.29 ± 0.03	0.30 ± 0.50	0.32 ± 0.46	0.38 ± 0.56	0.48 ± 0.39	0.54 ± 0.18	0.65 ± 0.18
08-Mar	308_02	0.26 ± 0.02	0.22 ± 0.31	0.23 ± 0.30	0.27 ± 0.35	0.33 ± 0.27	0.33 ± 0.22	0.40 ± 0.23
09-Mar	309_01	0.29 ± 0.03	0.62 ± 0.37	0.77 ± 0.72	0.76 ± 0.74	0.76 ± 0.33	0.89 ± 0.76	0.97 ± 0.79
	309_02	0.29 ± 0.03	0.39 ± 0.28	0.44 ± 0.39	0.49 ± 0.42	0.42 ± 0.37	0.47 ± 0.30	0.51 ± 0.31
12-Mar	312_01*	0.31 ± 0.03	0.32 ± 0.34	0.31 ± 0.28	0.32 ± 0.31	0.31 ± 0.20	0.30 ± 0.09	0.32 ± 0.10
	312_03*	0.39 ± 0.03	0.32 ± 0.53	0.32 ± 0.49	0.33 ± 0.54	0.39 ± 0.26	0.39 ± 0.11	0.42 ± 0.12
13-Mar	313_01*	0.28 ± 0.02	0.15 ± 0.20	0.13 ± 0.19	0.13 ± 0.18	0.22 ± 0.15	0.20 ± 0.09	0.20 ± 0.09
	313_02*	0.41 ± 0.04	0.74 ± 0.63	0.80 ± 0.60	0.91 ± 0.66	0.84 ± 0.60	0.83 ± 0.36	0.97 ± 0.37
	313_03	0.47 ± 0.04	0.08 ± 0.16	0.09 ± 0.18	0.09 ± 0.18	0.06 ± 0.06	0.08 ± 0.08	0.07 ± 0.08
	313_04	0.48 ± 0.04	0.13 ± 0.12	0.14 ± 0.08	0.13 ± 0.09	0.14 ± 0.11	0.14 ± 0.08	0.13 ± 0.08
	313_05	0.52 ± 0.05	0.24 ± 0.34	0.24 ± 0.32	0.20 ± 0.28	0.28 ± 0.21	0.29 ± 0.15	0.25 ± 0.16
14-Mar	314_01	0.26 ± 0.03	0.09 ± 0.08	0.09 ± 0.08	0.18 ± 0.12	0.10 ± 0.07	0.10 ± 0.07	0.17 ± 0.09
	314_02	0.45 ± 0.05	0.02 ± 0.03	0.03 ± 0.03	0.04 ± 0.02	0.05 ± 0.02	0.02 ± 0.03	0.02 ± 0.04
	314_03	0.68 ± 0.03	0.40 ± 0.43	0.46 ± 0.48	0.26 ± 0.51	0.40 ± 0.35	0.47 ± 0.36	0.24 ± 0.45
NMAE** [%]			53.86	57.16	58.20	64.59	68.29	71.48
Bias [%]			−1.06	3.68	5.63	17.56	21.69	23.27
RMSE [%]			68.60	73.07	75.71	81.14	86.48	89.35
Optimal measurement condition	NMAE [%]		28.56	30.41	29.63	53.68	55.26	51.73
	Bias [%]		11.44	12.05	11.90	48.34	47.53	44.35
	RMSE [%]		38.66	38.40	37.88	79.55	77.95	70.48
Non optimal measurement conditions	NMAE [%]		74.11	78.55	81.05	73.31	78.70	87.27
	Bias [%]		−11.06	−3.02	0.61	−7.06	1.02	6.41
	RMSE [%]		85.29	91.83	95.76	82.40	92.74	101.97

Flight codes with * are measurement flights with optimal conditions in terms of meteorology and downwind distance described in Section 5.2.2. **NMAE: Normalize mean absolute error.

Table S2. Altitude drift of UAV-GPS compared to RTK-GPS

Fl. Code	Drift $[\mathrm{cm\,s^{-1}}]$	Release Rate	RTK-Estimate $[\mathrm{g\,s^{-1}}]$	UAV-Estimate $[\mathrm{g\,s^{-1}}]$
309_02	0.01 ± 0.54	0.29 ± 0.03	0.39 ± 0.28	0.38 ± 0.22
312_01	0.21 ± 0.67	0.31 ± 0.03	0.32 ± 0.34	0.31 ± 0.24
312_03	0.02 ± 0.82	0.39 ± 0.03	0.32 ± 0.53	0.29 ± 0.38
313_01	0.12 ± 0.72	0.28 ± 0.02	0.15 ± 0.20	0.15 ± 0.17
313_02	0.17 ± 0.67	0.41 ± 0.04	0.82 ± 0.77	0.82 ± 0.66
313_03	0.04 ± 0.81	0.47 ± 0.04	0.08 ± 0.16	0.08 ± 0.18
313_04	0.05 ± 0.80	0.48 ± 0.04	0.13 ± 0.12	0.15 ± 0.13
313_05	0.17 ± 0.75	0.52 ± 0.05	0.24 ± 0.34	0.28 ± 0.29
314_01	0.13 ± 0.56	0.26 ± 0.03	0.09 ± 0.08	0.09 ± 0.07
314_02	0.21 ± 0.46	0.45 ± 0.05	0.02 ± 0.03	0.02 ± 0.03
314_03	0.11 ± 0.40	0.68 ± 0.03	0.40 ± 0.43	0.42 ± 0.45

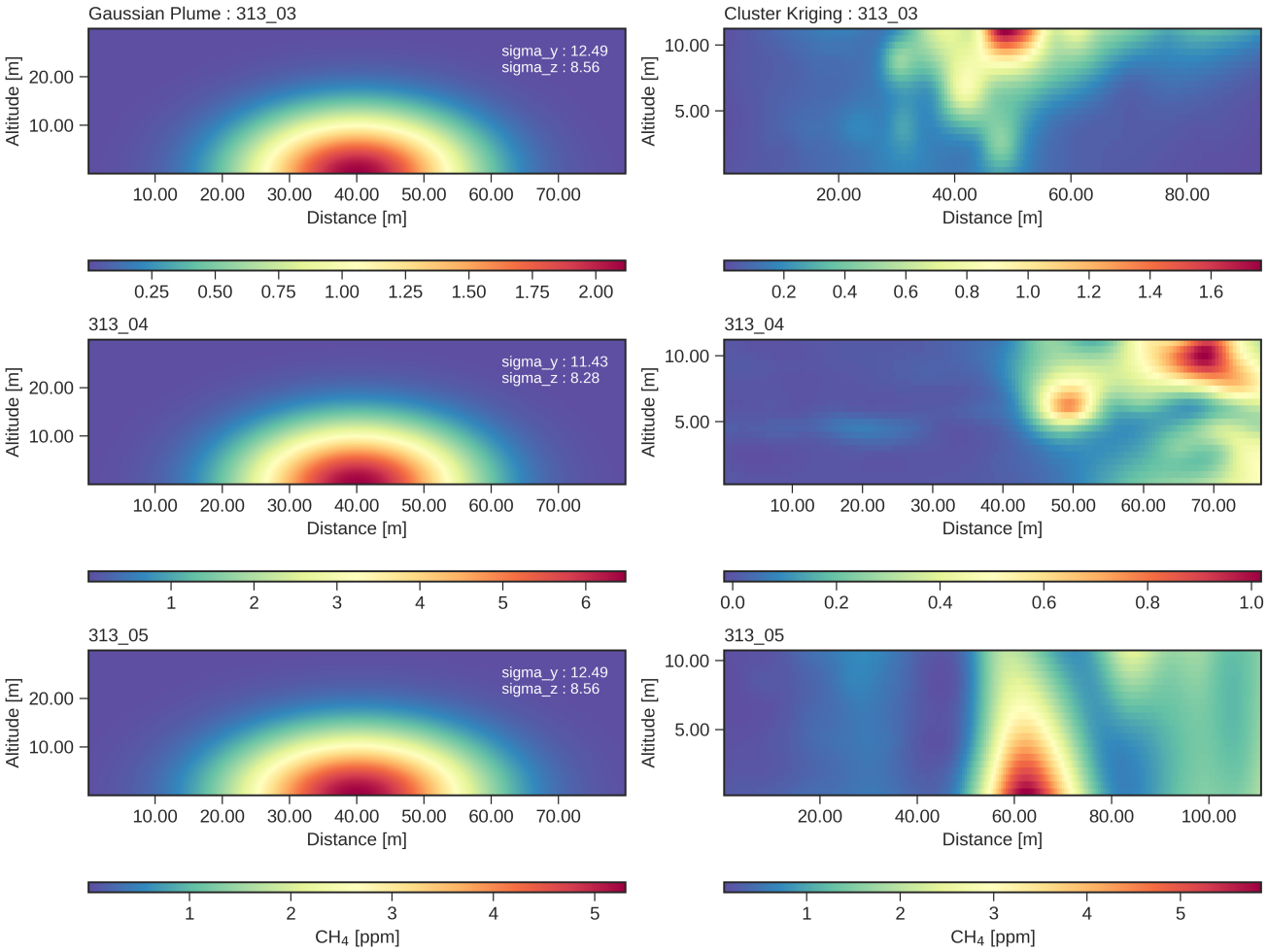

Figure S3. Vertical cross-section methane molar fractions generated using a theoretical Gaussian dispersion model and cluster-kriging estimated prediction at low wind speeds ($< 1\,\mathrm{ms}^{-1}$)

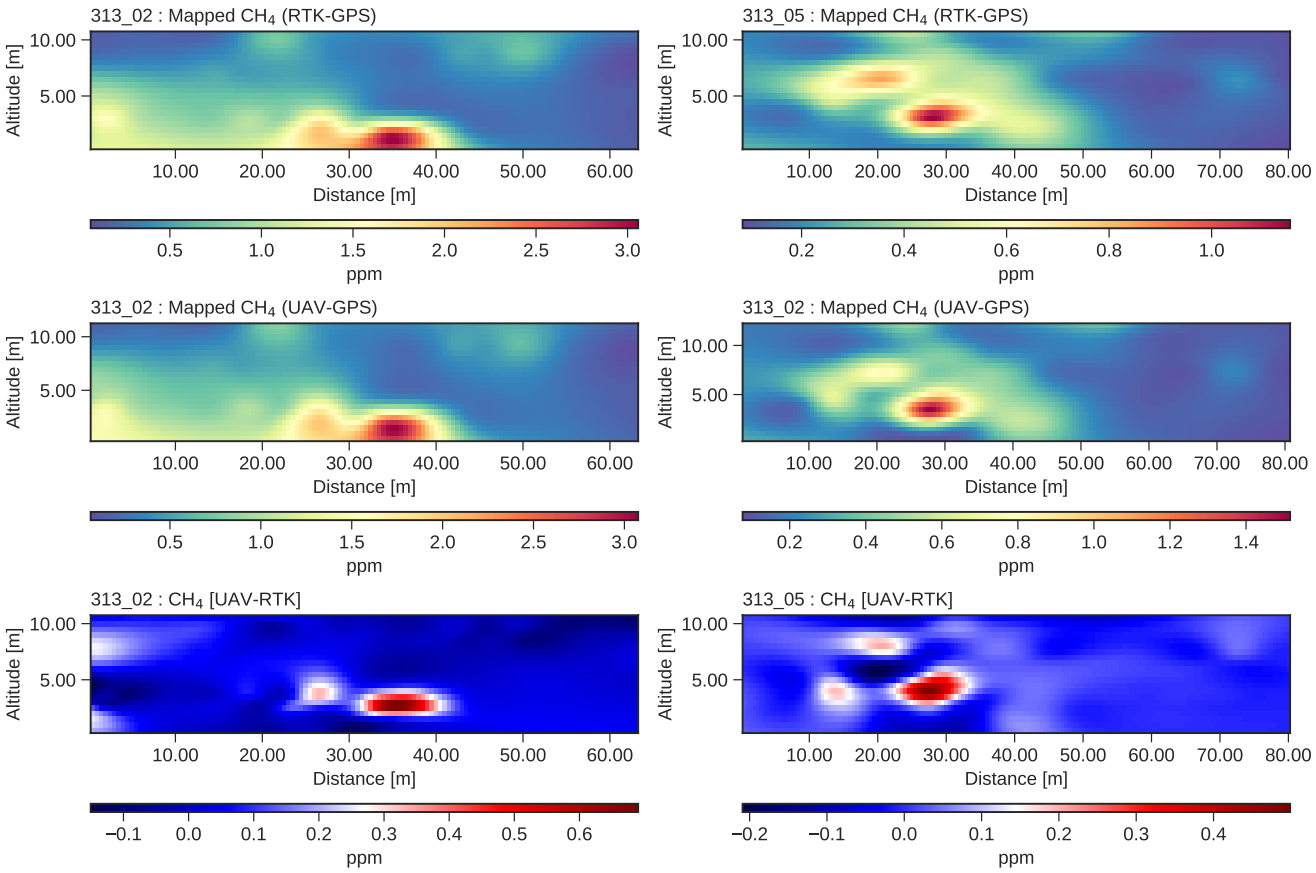

Figure S4. Mapped methane plume for flights 313_02 and 313_05 using RTK-GPS and UAV-GPS. The difference between the methane mole fraction field is also shown.

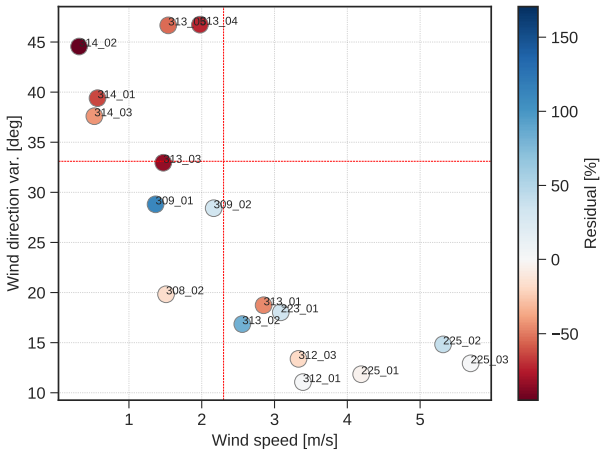

Figure S5. Residual plot between true and estimated release with respect to mean wind speed and directional variability. The circles in the lower right corner correspond to the eight out of 18 flights that meet the prescribed threshold. Residual errors characterized by light red and blue colors are generally lower for these flights.

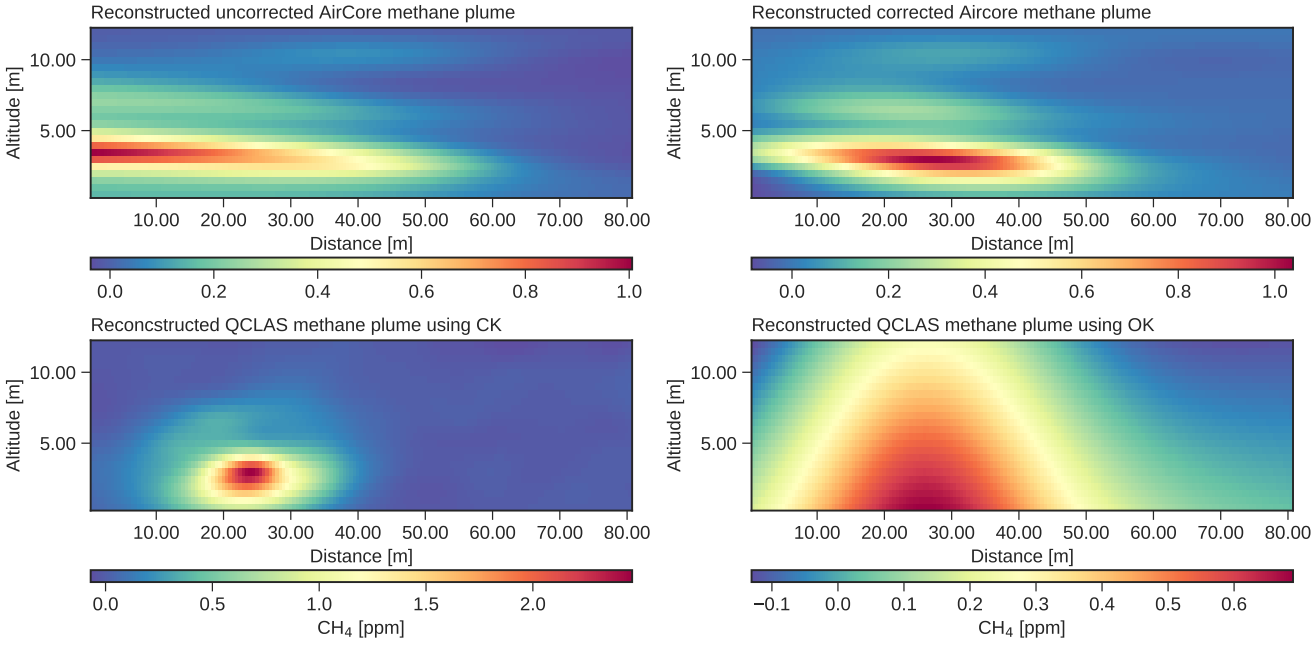

Figure S6. Reconstructed methane plume for flight 312_03. The figure on the upper left shows a reconstructed plume without applying a proper time correction for AirCore measurements, whereas the figure on the upper right is a reconstructed plume obtained after applying the proper time correction. The two bottom figures shows the reconstructed plume using the QCLAS measurement. After applying the proper correction, the methane plume moved spatially to the right placing it towards the center of the mapping plane. This resulted to a 23 % increase in emission estimate—closer to the true release.

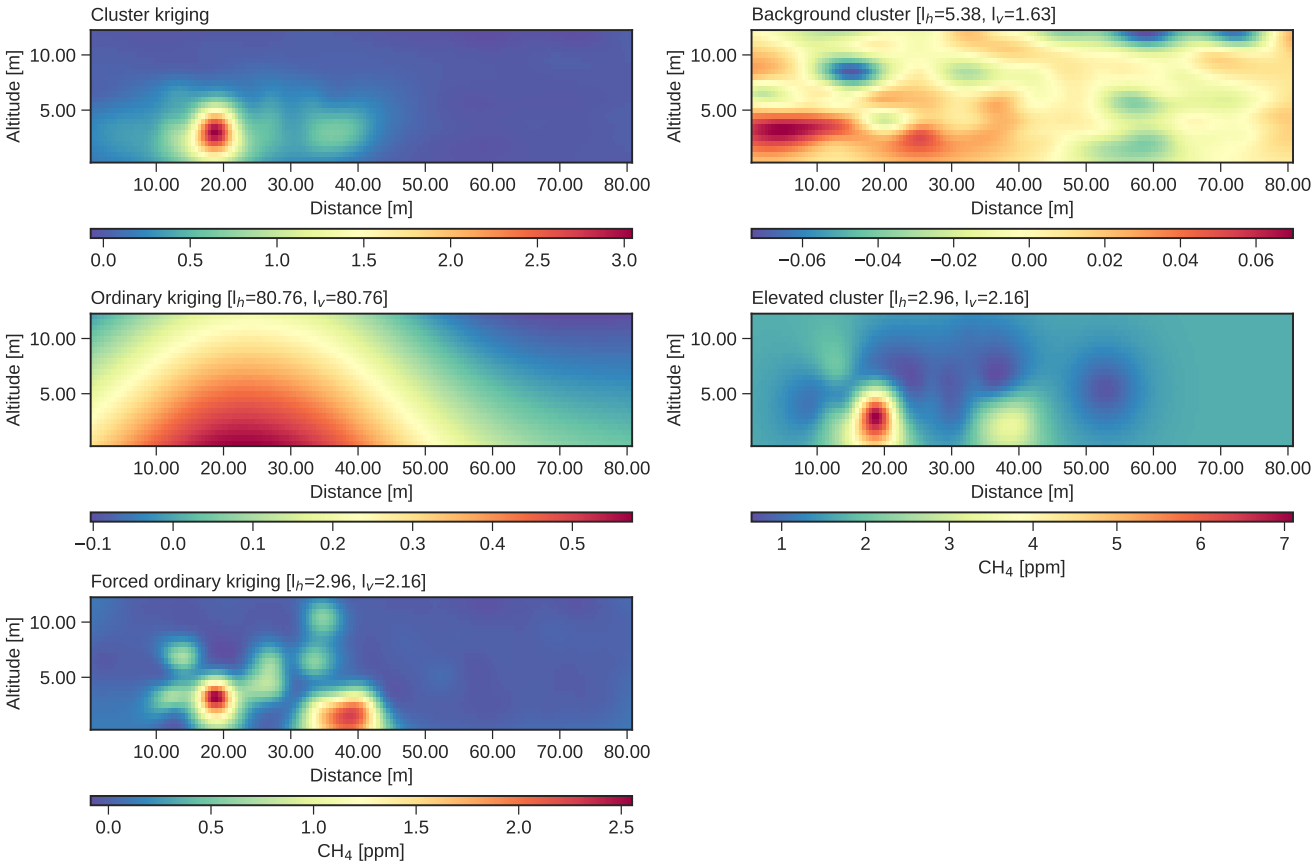

Figure S7. Reconstructed methane plume for 312_03 from QCLAS measurements using cluster-based vs ordinary kriging. Length scales written on top of each plot. Horizontal length scale is l_h while vertical length scale is l_v.